Published in final edited form as:
Cell Commun Adhes. 2008 September ; 15(3): 289–303. doi:10.1080/15419060802198736.

Connexin43 Expression Levels Influence Intercellular Coupling and Cell Proliferation of Native Murine Cardiac Fibroblasts

Yan Zhang[1,2], **Evelyn M. Kanter**[1,2], **James G. Laing**[1,2], **Colette Aprhys**[3], **David C. Johns**[3], **Elissavet Kardami**[4], and **Kathryn A. Yamada**[1,2,5]

1*Department of Medicine, Cardiovascular Division, Washington University School of Medicine*

2*Center for Cardiovascular Research, Washington University School of Medicine*

3*Department of Neurosurgery, Johns Hopkins School of Medicine*

4*Departments of Human Anatomy and Cell Sciences and Physiology and the Institute of Cardiovascular Sciences, University of Manitoba*

Abstract

Little is known about connexin expression and function in murine cardiac fibroblasts. We isolated native ventricular fibroblasts from adult mice and determined that although they expressed both connexin43 (Cx43) and connexin45 (Cx45), the relative abundance of Cx45 was greater than that of Cx43 in fibroblasts compared to myocytes, and the electrophoretic mobility of both Cx43 and Cx45 differed in fibroblasts and in myocytes. Increasing Cx43 expression by adenoviral infection increased intercellular coupling, while decreasing Cx43 expression by genetic ablation decreased coupling. Interestingly, increasing Cx43 expression reduced fibroblast proliferation, while decreasing Cx43 expression increased proliferation. Our data demonstrate that native fibroblasts isolated from the mouse heart exhibit intercellular coupling via gap junctions containing both Cx43 and Cx45. Fibroblast proliferation is inversely related to the expression level of Cx43. Thus, connexin expression and remodeling is likely to alter fibroblast function, maintenance of the extracellular matrix and ventricular remodeling in both normal and diseased hearts.

Keywords

connexin; Cx43; Cx45; murine; cardiac fibroblast; proliferation

INTRODUCTION

Cardiac fibroblasts form a 3-dimensional cellular network surrounding myocytes [Goldsmith et al. 2004], and contribute to myocardial structure by maintaining and remodeling the extracellular matrix in healthy and diseased hearts [Camelliti et al. 2005]. Recently, reports describing direct electrical coupling between cardiac fibroblasts and myocytes in culture demonstrate that fibroblasts bridging a discontinuous myocyte strand can conduct continuous electrical impulses [Miragoli et al. 2006; Gaudesius et al. 2003]. However, propagation velocity is slowed across the fibroblast bridge. Thus, fibroblasts may influence cardiac function not only by extracellular matrix remodeling [Eghbali et al 1989; Cleutjens et al. 1994], but also by modulating active and passive electrical properties, and thereby influencing (slowing) impulse propagation. Heterocellular coupling between fibroblasts and myocytes, although readily

5 Address correspondence to: Kathryn A. Yamada, Ph.D., Cardiovascular Division, Box 8086, Washington University School of Medicine, 660 South Euclid Avenue, St. Louis, MO 63110, Telephone: 314-362-8909, FAX: 314-362-8957, e-mail: kyamada@wustl.edu.

demonstrable in vitro, has been more difficult to show convincingly in situ. One reason for this may be that gap junctional plaques connecting fibroblasts alone or fibroblasts and myocytes are likely to be structurally more discrete and much smaller than those connecting myocytes.

Gap junctions of cardiac myocytes have been studied extensively. They are responsible for cell-to-cell communication, intercellular propagation of electrical signals and exchange of small signaling molecules throughout the heart. They are formed by individual connexins which exhibit different biophysical properties [Veenstra 1996]. Three connexins are expressed in cardiac myocytes found in ventricular myocardium. Cx43 is the predominant connexin expressed in working ventricular myocytes and is responsible for electrical coupling in the ventricles [Kanno and Saffitz 2001]. Cx45 and Cx30.2/31.9 are expressed primarily in the cardiac conduction system [Coppen et al. 1999; Bukauskas et al. 2006]. Gap junctions of cardiac fibroblasts, on the other hand, have been less extensively studied. Fibroblast gap junctions isolated from neonatal rat hearts are composed of Cx43 and Cx45 [Goldsmith et al. 2004; Miragoli et al. 2006; Gaudesius et al. 2003; Sundset et al. 2004]. Likewise, fibroblasts present in adult rabbit ventricular myocardium [Camelliti et al. 2005] and in healing infarcts in adult sheep [Camelliti et al. 2004a] express Cx43 and Cx45.

Fibroblasts play a critical role in ventricular remodeling, particularly post-myocardial infarction (MI). They migrate into damaged tissue and proliferate rapidly. They are arguably the most important component of the “living scar” [Sun et al. 2002], responsible for myocardial repair, infarct healing and scar formation. Indeed, Camelliti et al. found that connexin-expressing fibroblasts invading infarct regions after coronary occlusion were responsible for progression of the infarct [Camelliti et al. 2004a]. However, although mouse models of cardiac injury (e.g. MI) have been used extensively to delineate cellular mechanisms responsible for remodeling, little is known about the connexin expression pattern of murine cardiac fibroblasts and how connexin expression levels influence cardiac fibroblast function. The anti-proliferative (tumor suppressor) effects of Cx43 have been well described in transformed cells or carcinoma cell lines [Naus 2002]. However, it is not known whether primary cardiac fibroblasts exhibit these same effects. Thus, we undertook this study to test the hypothesis that (1) native murine cardiac fibroblasts express Cx43 and Cx45 and (2) changes in the expression level of Cx43 influence fibroblast function. We found that the relative abundance and electrophoretic mobility of Cx43 and Cx45 are different in fibroblasts than in myocytes. We also found that the expression level of Cx43 is an important determinant of intercellular coupling and proliferation of ventricular fibroblasts.

MATERIALS AND METHODS

Animals were handled in accordance with the NIH Guide for the Care and Use of Laboratory Animals; all protocols were approved by the Washington University Animal Studies Committee.

$Cx43^{+/+}$ and $Cx43^{+/-}$ Mice

We maintain a colony of wild-type ($Cx43^{+/+}$) mice and mice heterozygous for a Cx43 null allele ($Cx43^{+/-}$) for breeding in a standard barrier facility. Founder mice (C57BL/6J,129-$Gja1^{tm1Kdr}$) were originally purchased from Jackson Laboratories (Bar Harbor, ME), and were subsequently backbred into a C57BL/6J background. The genotypes of all mice were determined by polymerase chain reaction (PCR) as described previously [Johnson et al. 1999].

Adult Mouse Fibroblast Cultures

Fibroblasts were prepared from ventricles of $Cx43^{+/+}$ and $Cx43^{+/-}$ adult mice using a protocol described previously for isolation of neonatal ventricular myocytes [Zhuang et al. 2000; Pimentel et al. 2002]. Briefly, hearts were excised, the ventricles were minced, and the small tissue pieces were dissociated in Hanks' balanced salt solution (without Ca^{2+} and Mg^{2+}) containing 0.1% trypsin (Roche Applied Science, Indianapolis, IN) and 0.14% pancreatin (Sigma-Aldrich, St. Louis, MO). The dispersed cells were resuspended in Dulbecco's modified Eagle medium (Sigma) containing 10% fetal bovine serum, penicillin and streptomycin, and were plated overnight in culture flasks at 37°C in an atmosphere of room air supplemented with 95% O_2/5% CO_2. The next day, non-adherent cells were removed during a media change. Flasks containing fibroblasts were kept in culture for 7–10 days until they reached confluency. Fibroblasts were then removed with trypsin and plated at a density of 1.5×10^5 cells per well in 6-well plates and at a density of 4×10^4 cells per chamber on 4-chamber slides that had been coated with collagen (Type IV, 200 μg/mL, Sigma).

Myocyte Isolation

Adult mouse ventricular myocytes were obtained using enzymatic dissociation and mechanical dispersion as described previously [Xu et al. 1999; Guo et al. 1999]. Briefly, hearts were removed from anesthetized (2.5% Avertin) mice, mounted on a Langendorff apparatus and perfused retrogradely through the aorta with 0.1% collagenase (Worthington Biochemical Corp., Lakewood, NJ) in Earle's Balanced Salt Solution. The myocytes were dispersed by gentle trituration and brought up to physiological [Ca^{2+}] in M199 (Sigma).

Immunocytochemistry

Fibroblast cultures were fixed in 4% paraformaldehyde. For vimentin staining, cells were blocked in phosphate buffered saline (PBS) containing 0.1% Triton X-100 and 3% normal donkey serum (Jackson ImmunoResearch Laboratories Inc., West Grove, PA) for 30 min, then exposed to guinea pig anti-vimentin primary antibody (1:800, Progen Biotechnik, Heidelberg, Germany) at 4°C overnight, followed by washes and exposure to Alexa 488-conjugated donkey anti-guinea pig secondary antibody (1:1000, Molecular Probes/Invitrogen, Eugene, OR) for 2 hr.

For discoidin domain receptor 2 (DDR2), α-smooth muscle actin (α-SMA) and Cx43 immunostaining, tyramide signal amplification (TSA, NEN Life Science, Waltham MA) was used. The TSA procedure requires three major steps: (1) incorporation of horseradish peroxidase (HRP), (2) treatment with Biotinyl Tyramide Amplification Reagent (NEN), and (3) visualization with fluorophore-conjugated streptavidin as follows. Briefly, after endogenous peroxidase activity was quenched with 3% H_2O_2, cells were blocked in Tris-NaCl-Blocking reagent (TNB, NEN) for 30 min, then exposed to one of the following primary antibodies overnight at 4°C: goat anti-DDR2 (1:100, Santa Cruz Biotechnology, Inc., Santa Cruz, CA), mouse anti-α-SMA with HRP (used neat, Dako North America, Inc., Carpinteria, CA), or rabbit anti-Cx43 (1:400, Zymed/Invitrogen, Carlsbad, CA).

After staining with each respective primary antibody, the following procedures were used to accomplish TSA steps 1, 2 and 3 described above. For DDR2 staining, biotinylated donkey anti-goat secondary antibody (1:200, Jackson) was used, followed by streptavidin with HRP (1:300, NEN) (step 1). For α-SMA staining, as stated above, the primary antibody contained HRP (step 1). For Cx43 staining, EnVision™+ anti-mouse with HRP secondary antibody (neat, Dako) was used (step 1). Subsequently, slides were incubated in Biotinyl Tyramide Amplification Reagent (1:300, NEN) for 10 min (step 2), followed by Cy2- or Cy3-conjugated streptavidin (1:500, Jackson) for 30 min (step 3) and Hoechst nuclear stain (1:10,000, Cambrex Bioscience, Walkersville, MD) for 10 min for fluorescence visualization.

For cadherin staining, mouse anti-pan-cadherin (1:300, Sigma) followed by Cy3-conjugated goat anti-mouse secondary antibody (1:200, Jackson) was used.

Immunofluorescence images were photographed using an AxioCam digital camera attached to an Olympus BX60 microscope.

Immunoblot Analysis and Alkaline Phosphatase Assay

Cell extracts were prepared by homogenization (20 strokes) using a Duall 20 glass conical pestle (Kimble/Kontes, Vineland, NJ) and sonication (6×15 s, Cole-Parmer 8850, Cole-Parmer Instrument Co., Chicago, IL) in a buffer solution containing (mM): 1 $NaHCO_3$, 5 EDTA, 1 EGTA, pH 8.0; with the following protease inhibitors: 1 μM pepstatin, 100 nM aprotinin, 1 mM benzamidine, 1 mM iodoacetamide, 1 μM leupeptin, 1 mM phenylmethylsulfonyl fluoride. Proteins were resolved by SDS-polyacrylamide (10%) gel electrophoresis (SDS-PAGE) and transferred to nitrocellulose membranes for incubation with rabbit anti-Cx43 (1:5000, Zymed), protein A-purified rabbit anti-Cx45 (1:4000, generous gift from T. Steinberg, Washington University, St. Louis, MO), rabbit anti-Cx43 phospho-specific (Ser368) (1:500, Cell Signaling/Upstate USA, Inc., Charlottesville, VA), rabbit anti-Cx40 (1:1000, Chemicon/Millipore, Temecula, CA), goat anti-vimentin (1:2500, Sigma), goat anti-actin (1:1000, Santa Cruz), and mouse anti-GAPDH (1:5000, Research Diagnostics, Inc./Fitzgerald Industries, Int., Concord, MA) primary antibodies. HRP-conjugated goat anti-rabbit (1:10,000, Jackson), donkey anti-goat (1:20,000, Santa Cruz), and sheep anti-mouse (1:10,000, Amersham/GE Healthcare Bio-sciences Corp., Piscataway, NJ) were used as secondary antibodies. Protein bands were visualized using Western Lightning Chemiluminescence Reagent Plus (Perkin Elmer LAS, Boston, MA). Immunoblots were quantified by densitometric analysis using Adobe Photoshop.

In some experiments, cell extracts were incubated in the presence (0.1 U/μg protein) or absence of alkaline phosphatase (Roche) at 37°C in a shaking water bath for 3 hr. Samples were then subjected to immunoblot analysis as described above.

Adenoviral-Induced Overexpression of Cx43

Adult cardiac fibroblasts were exposed for 2 hr to adenoviral Cx43 (AdVCx43) [Doble et al. 2004] or a control adenoviral construct containing a CMV promoter [Hoppe et al. 2000] 24 hr after plating at an MOI of 50–100 and allowed to recover at 37°C for 4–5 days before being used in dye transfer experiments, or for 24 hr before being used in immunoblotting experiments.

Dye-Transfer Assay

Cells grown on 4-chamber slides were rinsed in phosphate buffered saline (PBS) and then incubated in PBS containing Lucifer yellow dye (2%, Sigma). A small circular glass-cutting tool was used to make a linear cut across the fibroblast monolayer to permit the membrane-impermeant dye to enter the damaged cells on either side of the scrape line (scrape-loading of dye) [El-Fouly et al. 1987]. After incubation for 2 min at 37°C, the monolayers were rinsed three times with PBS, fixed in 4% paraformaldehyde, mounted, and photographed using a fluorescence microscope and Nikon Coolpix 995 camera. Digital images were analyzed off-line using ImageJ software (NIH, http://rsb.info.nih.gov/ij/). An investigator blinded to genotype or treatment (Y.Z.) summated the area of fluorescence on one side of the scrape line and then divided the area by the length of the field to get an average distance of dye transfer, expressed in micrometers according to equation 1.

$$\text{Dye transfer } (\mu\text{m}) = \sum \text{area}(\mu\text{m}^2)/\text{length of field } (\mu\text{m}) \quad (1)$$

Two to 5 fields from each chamber were averaged. At least 2 different chambers of cells were plated from each heart. N's are the number of different hearts analyzed.

Fibroblast Proliferation

Fibroblasts were seeded in 96-well plates at a density of 1×10^4 cells per well. Cells were incubated at 37°C for 24 hr, then treated with 10 μM bromo-deoxyuridine (BrdU, Roche) for 16–24 hr. DNA synthesis was assessed using a colorimetric cell proliferation ELISA (Roche) according to the manufacturer's instructions and was used as a surrogate measure for cardiac fibroblast proliferation. Absorbance of the samples was measured in a spectrophotometer at 450 nm (reference wavelength 650 nm) with stop solution as reported by Wang et al. [Wang et al. 2002]. N's are the number of individual wells per genotype or cell treatment.

Statistical Analysis

All values are expressed as mean ± S.D. Two group comparisons were made using Student's t-test for grouped data. A value of $p < 0.05$ was considered significant.

RESULTS

All adult murine cardiac fibroblasts used in the present study were obtained after a single passage. Fibroblasts obtained from second or third passages appeared to undergo differentiation, exhibited altered morphology and produced a collagen matrix that interfered with dye transfer and immunostaining experiments. Cells from passage 1 grew to confluency within 4 or 5 days after plating. All cells stained positive for vimentin (Figure 1). Widespread expression of the fibroblast specific marker, DDR2, confirmed that the fibroblast cultures were nearly pure (Figure 1). A subset (<10%) of fibroblasts expressed α-SMA typical of myofibroblasts (Figure 1).

Adult Mouse Cardiac Fibroblasts Exhibit a Distinct Connexin Expression Pattern Compared to Cardiac Myocytes

Immunoblot analysis showed that adult murine fibroblasts expressed both Cx43 and Cx45 (Figure 2). Fibroblasts expressed less Cx43 than did myocytes isolated from the same hearts. Cx45 abundance was greater in adult mouse cardiac fibroblasts than in adult myocytes. We used the protein bands (40–45 kD) in the dried gel to normalize the connexin protein values obtained in Figure 2. Cx43 expression was significantly ($p < 0.001$) lower in fibroblasts compared to myocytes. Cx45 expression was not significantly different ($p = 0.205$) between the two cell types. As expected, vimentin and actin expression were differentially expressed in fibroblasts and myocytes, respectively (Figure 2). We also calculated the ratio of Cx45 to Cx43 band densities (from the same immunoblot membranes) to illustrate the difference in connexin expression in the two cell types (Figure 2). The ratio of Cx45 to Cx43 expression levels in fibroblasts was significantly greater than that in myocytes. Cx40 could not be detected in cardiac fibroblast cultures (data not shown).

We examined Cx43 expression by immunofluorescence microscopy. The immunostaining pattern of Cx43 expression in fibroblasts was markedly different from the appositional membrane staining typically observed in myocytes. Punctate staining was observed throughout the fibroblast cultures (Figure 1). However, gap junctional plaques represented by appreciable immunoreactive signal concentrated at intercellular junctions were not observed. In contrast, immunostaining for cadherins using an anti-pancadherin antibody was observed at all intercellular junctions and demonstrated that cell-cell contact and adhesion was maintained in these cultures (Figure 1).

Phosphorylation of Cx43 and Cx45 in Cardiac Fibroblasts

We observed a difference in electrophoretic mobility of Cx43 isolated from fibroblasts versus myocytes, suggesting that the phosphorylation status of Cx43 differs in fibroblasts compared to myocytes (Figure 2). Fibroblasts express Cx43 detected on immunoblots as protein bands at 41–46 kD. However, the majority (60%) of Cx43 signal in the fibroblast lanes was present in a faster migrating band at 41 kD (0.6 ± 0.1 density at 41 kD/total density at 41–46 kD, n = 7). The 41 kD band is also known as the nonphosphorylated, or NP, Cx43 band. In contrast, the major Cx43 bands in the myocyte lanes were the phosphorylated, or P1 and P2, bands migrating at ~44–46 kD. Only a minority (20%) of Cx43 signal in the myocyte lanes was present at 41 kD (0.2 ± 0.1 density at 41 kD/total density at 41–46 kD, n = 7). This difference in the 41 kD band density between fibroblasts and myocytes was statistically significant ($p<0.001$). However, both fibroblast and myocyte Cx43 was phosphorylated on ser368, as detected by a specific anti-phospho(ser368)Cx43 antibody (Figure 2). Anti-phospho(ser368)-Cx43 antibodies recognize a band that migrates at 41 kD [Solan et al. 2003]. Therefore, the faster migrating 41 kD band does not consist of nonphosphorylated species exclusively.

To confirm that the 44–46 kD bands represented phosphorylated Cx43, we incubated tissue extracts with alkaline phosphatase and demonstrated that Cx43 is phosphorylated in both fibroblasts and myocytes (Figure 3). Alkaline phosphatase treatment abolished the slower migrating P1 and P2 bands in both cell types.

Interestingly, Cx45 isolated from fibroblasts migrated faster than Cx45 from myocytes (Figure 2). We incubated tissue extracts from both fibroblasts and myocytes with alkaline phosphatase. Alkaline phosphatase treatment did not change the migration pattern of Cx45 in either fibroblasts or myocytes (Figure 3), suggesting that the difference in electrophoretic mobility of Cx45 in fibroblasts versus myocytes is not due to a difference in phosphorylation status.

Cx43-Deficient Fibroblasts Exhibit Reduced Intercellular Coupling

We isolated adult cardiac fibroblasts and measured Cx43 and Cx45 expression levels in fibroblasts cultured from both $Cx43^{+/-}$ and wild-type mice (Figure 4). As expected, Cx43 expression was reduced significantly ($p=0.024$) by 50% in $Cx43^{+/-}$ fibroblasts (0.5 ± 0.3 relative density units, n = 7) compared to $Cx43^{+/+}$ cells (1.0 ± 0.5 relative density units, n = 8). Cx45 expression was comparable in $Cx43^{+/-}$ and $Cx43^{+/+}$ fibroblasts (1.0 ± 0.4 and 1.0 ± 0.3 units, respectively, $p = 0.881$). Intercellular coupling was assessed by Lucifer yellow dye transfer. Wild-type fibroblast cultures exhibited a consistent level of intercellular coupling (Figure 4C, left and 4D) despite a lack of distinct Cx43 staining at appositional membranes, indicating that intercellular communication between cardiac fibroblasts takes place through gap junctions that are smaller than and not as readily detectable as their myocyte counterparts. Cell-to-cell dye transfer was reduced significantly ($p = 0.018$) in $Cx43^{+/-}$ (64 ± 7 μm) compared to control wild-type (84 ± 19 μm) cardiac fibroblasts (n = 7 chambers each) as shown in Figure 4.

Cx43-Overexpressing Fibroblasts Exhibit Enhanced Intercellular Coupling

To investigate further whether altering connexin expression would change coupling, we treated wild-type adult cardiac fibroblasts with either an adenoviral construct (MOI of 50–100) to increase Cx43 expression or a control adenoviral construct (MOI of 50–100). Two hours of AdVCx43 infection at an MOI of 100 resulted in an ~60% increase in Cx43 over control values (Figure 5). Increased expression of Cx43 resulted in significantly ($p = 0.008$) greater dye transfer in AdVCx43-infected fibroblasts (101 ± 10 μm) compared to control adenovirus-infected wild-type cells (64 ± 3 μm, n = 3 chambers each) as shown in Figure 5.

Cx43 Expression Levels Influence Fibroblast Proliferation

Finally, we assessed the influence of Cx43 expression levels on proliferative activity in our fibroblast cultures using a DNA synthesis assay. Fibroblast proliferation was increased significantly ($p<0.001$) in Cx43-deficient (1.49 ± 0.21 relative OD units) compared to wild-type (1.20 ± 0.17 units) fibroblast cultures ($n = 24$) as shown in Figure 6. Furthermore, proliferation was decreased significantly ($p<0.001$) in AdVCx43-infected cultures overexpressing Cx43 (1.20 ± 0.15 units) compared to control adenovirus-infected wild-type (1.85 ± 0.18 units) cultures ($n = 23$) as shown in Figure 6. Thus, reducing Cx43 expression increases cardiac fibroblast proliferation and increasing Cx43 expression inhibits cardiac fibroblast proliferation.

DISCUSSION

The present study was conducted on primary fibroblast cultures in vitro to directly compare connexin expression patterns in relatively pure populations of cardiac fibroblasts versus myocytes. Our results point to three novel findings that have not been reported previously in primary fibroblasts isolated directly from adult mouse hearts. First, native murine ventricular fibroblasts express both Cx43 and Cx45; however, their relative abundance and electrophoretic mobility are different from that of myocytes. Second, the level of Cx43 expression is a determinant of intercellular coupling of fibroblasts. Third, Cx43 expression levels influence the proliferative activity of cardiac fibroblasts.

Connexin Expression Patterns in Adult Ventricular Fibroblasts

Cx43 and Cx45 are the predominant gap junction proteins in ventricular myocardium. We found that the primary molecular species of connexin proteins (both Cx43 and Cx45) expressed in fibroblasts are structurally different from those expressed in myocytes. In myocytes, the major Cx43 bands are slower migrating 44–46 kD P1 and P2 bands, whereas the major Cx43 band from fibroblasts is the more rapidly migrating 41 kD NP band. Thus, the phosphorylation status of Cx43 appears to be different in cardiac fibroblasts compared with myocytes. However, following alkaline phosphatase treatment, the slower migrating forms from both myocytes and fibroblasts (Figure 3) collapsed to the 41 kD form, suggesting that phosphorylation is the primary covalent modification detected by immunoblotting in both cell types. We also found that fibroblast Cx43 is phosphorylated on ser368 (Figure 2).

The significance of phosphorylation of Cx43 at ser368 and reduced P1 and P2 bands from fibroblasts is not clear at the present time. Up to 16 sites on the carboxyl-terminus of Cx43 can be phosphorylated [Axelsen et al. 2006]. The effects of phosphorylation are complex. In many systems phosphorylation of Cx43 by protein kinase C regulates its degradation and either increases or inhibits gap junction communication [Lampe and Lau 2004]. This may be the case in both fibroblasts and myocytes. Recently, however, Lampe et al. reported a correlation between phosphorylation at ser325/ser328/ser330 (which migrates as the P2 band) with efficient gap junction formation and function [Lampe et al. 2006]. The reduced abundance of the P1 and P2 forms of Cx43 in our fibroblasts compared to myocytes may account for reduced gap junction formation in our fibroblast cultures. However, as shown by Lampe et al., mutants lacking the ser325/ser328/ser330 phosphorylation sites can still form functional gap junctions, albeit to a lesser extent [Lampe et al. 2006]. We did not specifically address the extent of phosphorylation at ser325/ser328/ser330, nor do we know how phosphorylation at ser368 may have contributed to coupling in our cultures. Clearly, additional studies will be required to determine which specific phosphorylation sites, or combination thereof, are critical for gap junctional communication in native cardiac fibroblasts.

Furthermore, Cx45 from native fibroblasts also exhibited faster electrophoretic mobility compared to that from myocytes. The reason for this difference is not known. Our data suggest that the faster migration pattern of Cx45 protein derived from fibroblasts is not due to altered phosphorylation between fibroblasts and myocytes. Although Cx45 is known to be a phosphoprotein [Laing et al. 1994; Hertlein et al. 1998], relatively little is known about the residues that are phosphorylated in myocytes, let alone in fibroblasts. Future studies designed to delineate post-translational modifications of connexin proteins using mass spectrometry and peptide sequencing from Cx43 and Cx45 immunoprecipitated from fibroblast cell extracts are warranted.

Connexin Expression Levels are a Determinant of Gap Junctional Communication in Adult Ventricular Fibroblasts

Our native cardiac fibroblast cultures exhibited diffuse, punctate Cx43 immunoreactive signal (Figure 1). We did not expect to find the large intercellular gap junctions that are typical of cardiac myocytes, as gap junctions in fibroblasts are typically small [De Maziere et al. 1992]. The punctate cytosolic staining may represent intracellular pools of nascent or recycled Cx43 protein. Nevertheless, we found that our cells were functionally well coupled. Taken together, our data are consistent with previously reported observations that cell types which make small gap junctional plaques that are hard to visualize by immunofluorescence microscopy still allow for gap junctional communication [Musil et al. 2000]. Our data also demonstrate that the extent of intercellular coupling of cardiac fibroblast cultures depends, at least in part, on the level of Cx43 expression. Decreasing or increasing the expression level of Cx43 either reduced or enhanced dye transfer in our fibroblast cultures, respectively, indicating that Cx43 expression levels are a determinant of intercellular coupling in these cells. The increase in Cx43 protein expression and coupling that we achieved with AdVCx43 was similar to that induced by basic fibroblast growth factor in primary rat cardiac fibroblasts [Doble and Kardami 1995] and in microvascular endothelial cells [Pepper and Meda 1992], suggesting that the levels of Cx43 expression in our cardiac fibroblast cultures are of physiological relevance.

Connexin Expression Levels Influence Proliferation of Adult Ventricular Fibroblasts

We found that there is an inverse relationship between the level of Cx43 expression and fibroblast proliferation. Reducing Cx43 expression enhanced fibroblast proliferation, and increasing Cx43 expression resulted in reduced fibroblast proliferation. Our data are unique in that our findings were demonstrated in primary cardiac cells. Our data are consistent with a large body of literature in transformed cells or stable cell lines delineating the anti-proliferative (tumor suppressor) effect of Cx43 [Naus 2002]. Zhang et al. [Zhang et al. 2003a; Zhang et al. 2003b] showed that Cx43 expression results in decreased S-phase kinase-associated protein 2 (Skp2) stability, increased cyclin-dependent kinase inhibitor, p27, and reduced cell proliferation. Whether this mechanism is operative in the cardiac fibroblast population has not been established. Furthermore, the relative contributions of gap junction dependent and independent mechanisms modulating fibroblast function remain to be elucidated.

Unanswered Questions Related to Gap Junction Communication in Adult Ventricular Fibroblasts

Additional unanswered questions have arisen from our data. Native fibroblasts isolated from adult mouse hearts express a significant amount of Cx45. The relative abundance of Cx45 to Cx43 is much greater in fibroblasts than in myocytes. We and others have shown that Cx45 expressed in gap junctions containing Cx43 significantly reduces intercellular coupling [Yamada et al. 2003; Koval et al. 1995]. We do not know whether the high expression level of Cx45 protein in fibroblasts may cause a diminution in gap junctional communication in these cells. Nor is it known whether high expression levels of Cx45 may contribute to smaller

gap junctional plaques in fibroblasts. Alternative explanations may account for the smaller, less extensive plaques observed in these cells. First, Cx43 gap junction formation is dependent on the presence of N-cadherin in the adherens junctions of the cell [Meyer et al. 1992; Musil et al. 1990]. Despite the fact that we observed robust expression of cadherins prominent at intercellular junctions, additional binding partners are required for plaque formation. Recently, Shaw et al. demonstrated that vesicles containing Cx43 bound for the plasma membrane dock at adherens junctions via interaction between microtubules, EB1, p150(Glued), β-catenin and N-cadherin [Shaw et al. 2007]. Therefore, a relative lack of expression of other adhesion molecules in fibroblasts may preclude abundant plaque formation compared to myocytes. Second, as discussed above, phosphorylation of Cx43 on ser325/ser328/ser330 by casein kinase 1 is crucial for gap junction assembly as well as efficient dye transfer [Lampe et al. 2006]. Thus, reduced phosphorylation at these residues may underlie smaller plaques in fibroblasts compared to myocytes.

Our data do not speak to the extent of heterocellular communication between fibroblasts and myocytes. Such coupling has been demonstrated conclusively in vitro [Miragoli et al. 2006; Gaudesius et al. 2003]. It has been more difficult to demonstrate convincingly in vivo [Camelliti et al. 2005]. Camelliti et al. reported that fibroblasts express Cx40 and Cx45 in sinoatrial nodal tissue and are coupled by Cx45 in regions of the node in which fibroblasts intermingle with myocytes [Camelliti et al. 2004b]. These investigators also demonstrated that intercellular junctions containing Cx43 and Cx45 may connect fibroblasts and myocytes in rabbit ventricular myocardium and within healing infarcts in sheep hearts [Camelliti et al. 2005; Camelliti et al. 2004a]. Additional studies will be required to establish the extent and functional role of heterocellular coupling in normal and diseased hearts, and whether there are differences in species ranging from mice to man.

The Expanding Role of Cardiac Fibroblasts

Although the main role of fibroblasts in the heart is considered to be synthesis and maintenance of the mechanical scaffold enveloping cardiac myocytes, it is increasingly appreciated that they also contribute to sensing and reacting to the changing milieu in the heart via communication with other resident cell types. Specifically, fibroblasts are capable of synchronizing electrical activity and may contribute to slow conduction in the heart [Miragoli et al. 2006; Gaudesius et al. 2003]. In addition, fibroblasts can detect environmental (e.g. chemical and mechanical) stimuli [Silzle et al. 2004; Smith et al. 1997]. Our data showing Cx43-dependent functional coupling of adult cardiac fibroblasts and modulation of fibroblast proliferation by varying Cx43 expression levels indicate that intercellular transport of metabolic and/or signaling molecules is influenced by changing levels of connexin expression in the heart. Therefore, connexin remodeling such as that observed after cardiac injury or during progression of cardiac disease is likely to affect the ability of fibroblasts to react to chemical and/or mechanical provocations. Fibroblast cultures isolated from various transgenic mice exhibiting specific phenotypes may be used to delineate the specific functions of native fibroblast populations to ultimately understand the complex array of diverse roles this important cell type plays in both healthy and diseased hearts.

Acknowledgements

The authors would like to thank Erin M. Gribben and Jefferson Gomes for expert technical help, Dr. Robert Heuckeroth for use of his fluorescence microscope and camera system, and Dr. Hongtao Wang for helpful discussions. This work was supported by an American Heart Association Fellowship to Y. Zhang, the Canadian Institutes for Health Research and the Heart and Stroke Foundation of Canada to E. Kardami, and NIH/NHLBI Grant HL-066350 to K.A. Yamada.

References

Axelsen LN, Stahlhut M, Mohammed S, Larsen BD, Nielsen MS, Holstein-Rathlou N-H, Andersen S, Jensen ON, Hennan JK, Kjølbye AL. Identification of ischemia-regulated phosphorylation sites in connexin43: a possible target for the antiarrhythmic peptide analogue rotigaptide (ZP123). J Mol Cell Cardiol 2006;40:790–798. [PubMed: 16678851]

Bukauskas FF, Kreuzberg MM, Rackauskas M, Bukauskiene A, Bennett MVL, Verselis VK, Willecke K. Properties of mouse connexin 30.2 and human connexin 31.9 hemichannels: implications for atrioventricular conduction in the heart. Proc Natl Acad Sci 2006;103:9726–9731. [PubMed: 16772377]

Camelliti P, Devlin GP, Matthews KG, Kohl P, Green CR. Spatially and temporally distinct expression of fibroblast connexins after sheep ventricular infarction. Cardiovasc Res 2004a;62:415–425. [PubMed: 15094361]

Camelliti P, Green CR, LeGrice I, Kohl P. Fibroblast network in rabbit sinoatrial node: structural and functional identification of homogeneous and heterogeneous cell coupling. Circ Res 2004b;94:828–835. [PubMed: 14976125]

Camelliti, Borg T, Kohl P. Structural and functional characterisation of cardiac fibroblasts. Cardiovasc Res 2005;65:40–51. [PubMed: 15621032]

Cleutjens JPM, Kandala JC, Guarda E, Guntaka RV, Weber KT. Regulation of collagen degradation in the rat myocardium after infarction. J Mol Cell Cardiol 1994;27:1281–1292. [PubMed: 8531210]

Coppen SR, Severs NJ, Gourdie RG. Connexin 45 (α6) expression delineates an extended conduction system in the embryonic and mature rodent heart. Dev Genet 1999;24:82–90. [PubMed: 10079513]

De Maziere AMGL, Van Ginneken ACG, Wilders R, Jongsma HJ, Bouman LN. Spatial and functional relationship between myocytes and fibroblasts in the rabbit sinoatrial node. J Mol Cell Cardiol 1992;24:567–578. [PubMed: 1518074]

Doble BW, Dang X, Ping P, Fandrich RR, Nickel BE, Jin Y, Cattini PA, Kardami E. Phosphorylation of serine 262 in the gap junction protein connexin-43 regulates DNA synthesis in cell-cell contact forming cardiomyocytes. J Cell Sci 2004;117:507–514. [PubMed: 14702389]

Doble BW, Kardami E. Basic fibroblast growth factor stimulates connexin-43 expression and intercellular communication of cardiac fibroblasts. Mol Cell Biochem 1995;143:81–87. [PubMed: 7776963]

Eghbali M, Blumenfeld OO, Seifter S, Buttrick PM, Leinwand LA, Robinson TF, Zern MA, Giambrone MA. Localization to types I, III and IV collagen mRNAs in rat heart cells by in situ hybridization. J Mol Cell Cardiol 1989;21:103–113. [PubMed: 2716064]

El-Fouly MH, Trosko JE, Chang C-C. Scrape-loading and dye transfer: a rapid and simple technique to study gap junctional intercellular communication. Exp Cell Res 1987;168:422–430. [PubMed: 2433137]

Gaudesius G, Miragoli M, Thomas SP, Rohr S. Coupling of cardiac electrical activity over extended distances by fibroblasts of cardiac origin. Circ Res 2003;93:421–428. [PubMed: 12893743]

Goldsmith EC, Hoffman A, Morales MO, Potts JD, Price RL, McFadden A, Rice M, Borg TK. Organization of fibroblasts in the heart. Dev Dyn 2004;230:787–794. [PubMed: 15254913]

Guo W, Xu H, London B, Nerbonne JM. Molecular basis of transient outward K^+ current diversity in mouse ventricular myocytes. J Physiol 1999;521:587–599. [PubMed: 10601491]

Hertlein B, Butterweck A, Haubrich S, Willecke K, Traub O. Phosphorylated carboxy terminal serine residues stabilize the mouse gap junction protein connexin45 against degradation. J Membrane Biol 1998;162:247–257. [PubMed: 9543497]

Hoppe UC, Marbán E, Johns DC. Adenovirus-mediated inducible gene expression in vivo by a hybrid ecdysone receptor. Mol Ther 2000;1:159–164. [PubMed: 10933926]

Johnson CM, Green KG, Kanter EM, Bou-Abboud E, Saffitz JE, Yamada KA. Voltage-gated Na^+ channel activity and connexin expression in Cx43-deficient myocytes. J Cardiovasc Electrophysiol 1999;10:1390–1401. [PubMed: 10515564]

Kanno S, Saffitz JE. The role of myocardial gap junctions in electrical conduction and arrhythmogenesis. Cardiovasc Pathol 2001;10:169–177. [PubMed: 11600334]

Koval M, Geist ST, Westphale EM, Kemendy EM, Civitelli R, Beyer EC, Steinberg TH. Transfected connexin45 alters gap junction permeability in cells expressing endogenous connexin43. J Cell Biol 1995;130:987–995. [PubMed: 7642714]

Laing JG, Westphale EM, Engelmann GL, Beyer EC. Characterization of the gap junction protein, connexin45. J Membrane Biol 1994;139:31–40. [PubMed: 8071985]

Lampe PD, Cooper CD, King TJ, Burt JM. Analysis of connexin43 phosphorylated at S325, S328 and S330 in normoxic and ischemic heart. J Cell Sci 2006;119:3435–3442. [PubMed: 16882687]

Lampe PD, Lau AF. The effects of connexin phosphorylation on gap junctional communication. Int J Biochem Cell Biol 2004;36:1171–1186. [PubMed: 15109565]

Meyer RA, Laird DW, Revel J-P, Johnson RG. Inhibition of gap junction and adherens junction assembly by connexin and A-CAM antibodies. J Cell Biol 1992;119:179–189. [PubMed: 1326565]

Miragoli M, Gaudesius G, Rohr S. Electrotonic modulation of cardiac impulse conduction by myofibroblasts. Circ Res 2006;98:801–810. [PubMed: 16484613]

Musil LS, Cunningham BA, Edelman GM, Goodenough DA. Differential phosphorylation of the gap junction protein connexin43 in junctional communication-competent and -deficient cell lines. J Cell Biol 1990;111:2077–2088. [PubMed: 2172261]

Musil LS, Le A-CN, VanSlyke JK, Roberts LM. Regulation of connexin degradation as a mechanism to increase gap junction assembly and function. J Biol Chem 2000;275:25207–25215. [PubMed: 10940315]

Naus CCG. Gap junctions and tumour progression. Can J Physiol Pharmacol 2002;80:136–141. [PubMed: 11934256]

Pepper MS, Meda P. Basic fibroblast growth factor increases junctional communication and connexin 43 expression in microvascular endothelial cells. J Cell Physiol 1992;153:196–205. [PubMed: 1325977]

Pimentel RC, Yamada KA, Kléber AG, Saffitz JE. Autocrine regulation of myocyte Cx43 expression by VEGF. Circ Res 2002;90:671–677. [PubMed: 11934834]

Shaw RM, Fay AJ, Puthenveedu MA, von Zastrow M, Jan Y-N, Jan LY. Microtubule plus-end-tracking proteins target gap junctions directly from the cell interior to adherens junctions. Cell 2007;128:547–560. [PubMed: 17289573]

Silzle T, Randolph GJ, Kreutz M, Kunz-Schughart. The fibroblast: sentinel cell and local immune modulator in tumor tissue. Int J Cancer 2004;108:173–180. [PubMed: 14639599]

Smith RS, Smith TJ, Blieden TM, Phipps RP. Fibroblasts as sentinel cells: synthesis of chemokines and regulation of inflammation. Am J Pathol 1997;151:317–322. [PubMed: 9250144]

Solan JL, Fry MD, TenBroek EM, Lampe PD. Connexin43 phosphorylation at S368 is acute during S and G_2/M and in response to protein kinase C activation. J Cell Sci 2003;116:2203–2211. [PubMed: 12697837]

Sun Y, Kiani MF, Postlethwaite AE, Weber KT. Infarct scar as living tissue. Basic Res Cardiol 2002;97:343–347. [PubMed: 12200633]

Sundset R, Cooper M, Mikalsen SO, Ytrehus K. Ischemic preconditioning protects against gap junctional uncoupling in cardiac myofibroblasts. Cell Commun Adhes 2004;11:51–66. [PubMed: 16247851]

Veenstra RD. Size and selectivity of gap junction channels formed from different connexins. J Bioenerg Biomembr 1996;28:327–337. [PubMed: 8844330]

Wang F, Trial J, Diwan A, Gao F, Birdsall H, Entman M, Hornsby P, Sivasubramaniam N, Mann DL. Regulation of cardiac fibroblast cellular function by leukemia inhibitory factor. J Mol Cell Cardiol 2002;34:1309–1316. [PubMed: 12392991]

Xu H, Guo W, Nerbonne JM. Four kinetically distinct depolarization-activated K^+ currents in adult mouse ventricular myocytes. J Gen Physiol 1999;113:661–678. [PubMed: 10228181]

Yamada KA, Rogers JG, Sundset R, Steinberg TH, Saffitz JE. Up-regulation of connexin45 in heart failure. J Cardiovasc Electrophysiol 2003;14:1205–1212. [PubMed: 14678136]

Zhang Y-W, Kaneda M, Morita I. The gap junction-independent tumor-suppressing effect of connexin 43. J Biol Chem 2003a;278:44852–44856. [PubMed: 12952975]

Zhang Y-W, Nakayama K, Nakayama K-I, Morita I. A novel route for connexin 43 to inhibit cell proliferation: negative regulation of S-phase kinase-associated protein (Skp 2). Cancer Res 2003b; 63:1623–1630. [PubMed: 12670914]

Zhuang J, Yamada KA, Saffitz JE, Kléber AG. Pulsatile stretch remodels cell-to-cell communication in cultured myocytes. Circ Res 2000;87:316–322. [PubMed: 10948066]

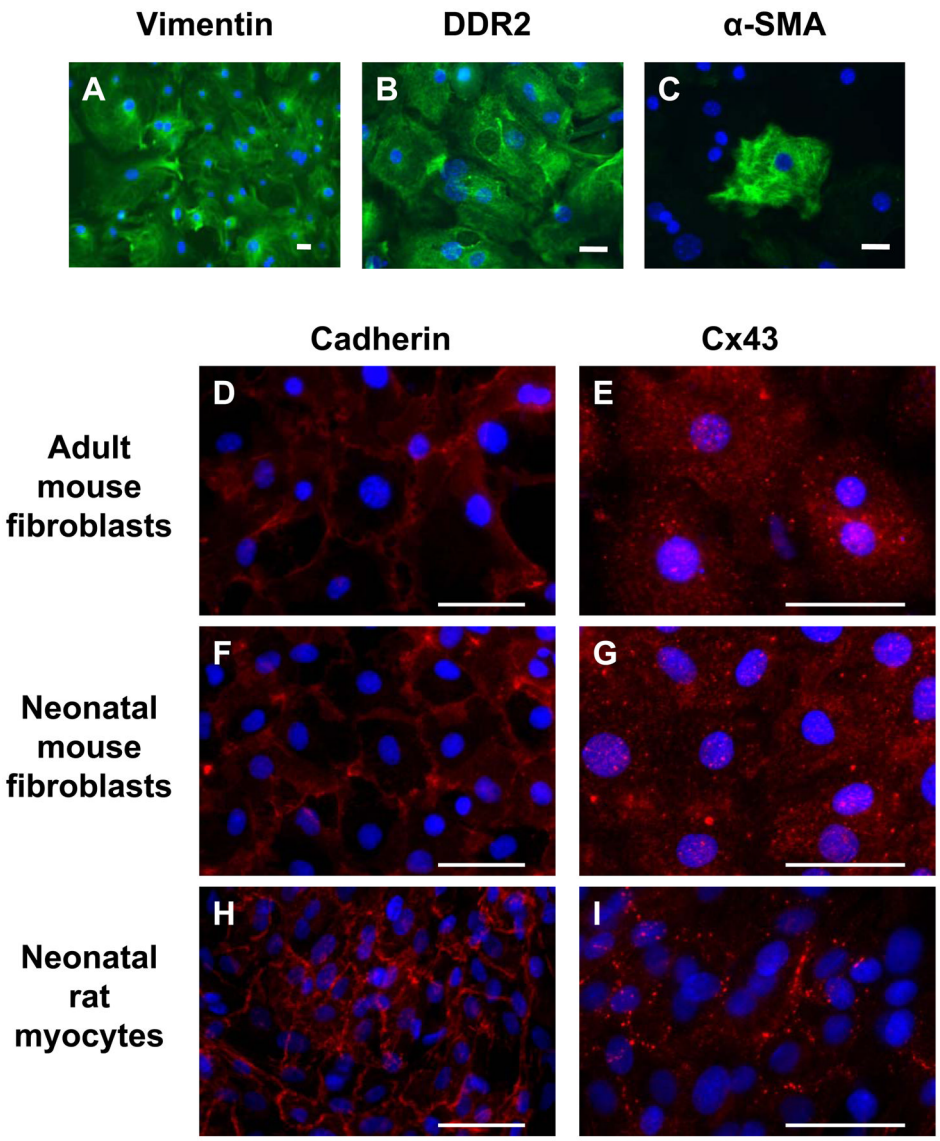

Figure 1.

Adult mouse cardiac fibroblast cultures express vimentin (A) and DDR2 (B). A subset of cells also expresses α-SMA (C). Cx43 signal is punctate and diffuse in both adult (E) and neonatal mouse fibroblasts (G). Neonatal rat myocytes exhibit the typical cardiac Cx43 staining at intercellular junctions (I). Pan-cadherin staining is evident at cell-cell junctions in each cell type (D, F, H). The limited appositional membrane staining in adult cardiac fibroblasts belies the fact that the fibroblast cultures are well coupled. Bar = 50 μm.

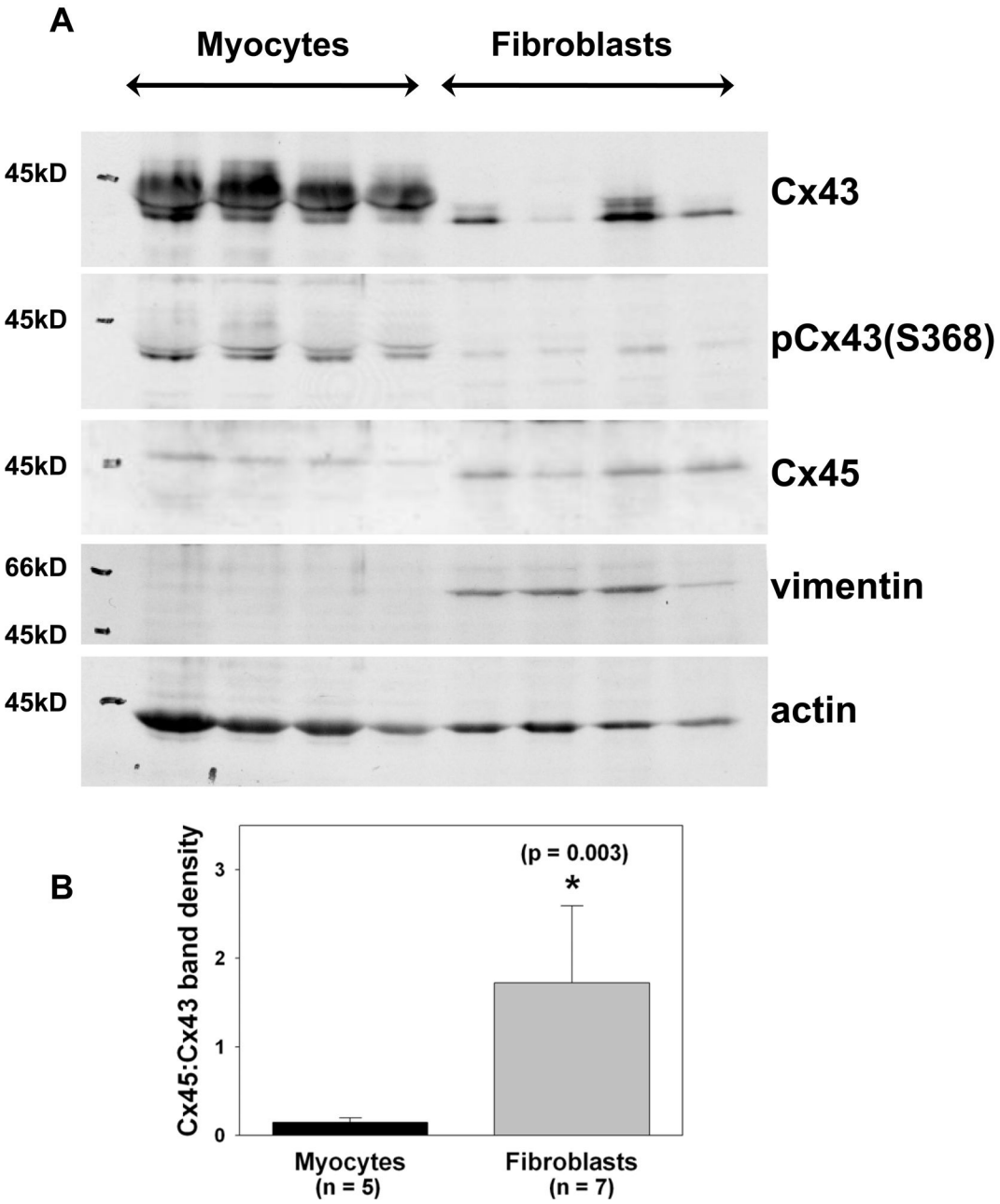

Figure 2.

Adult mouse cardiac fibroblasts express both Cx43 and Cx45. (A) The first four lanes represent adult myocyte extracts. The last four lanes represent adult fibroblast extracts. Equal protein (30 μg) was loaded in each lane. Fibroblasts express less Cx43 than myocytes. Cx45 is comparable in fibroblasts and myocytes, but Cx45 in fibroblasts migrated faster than that in myocytes. (B) Relative expression of Cx43 and Cx45 in adult cardiac myocytes and fibroblasts. The ratio of Cx45 to Cx43 band density obtained from myocytes isolated from 5 different hearts and fibroblasts obtained from 7 different hearts is significantly larger for fibroblasts than for myocytes.

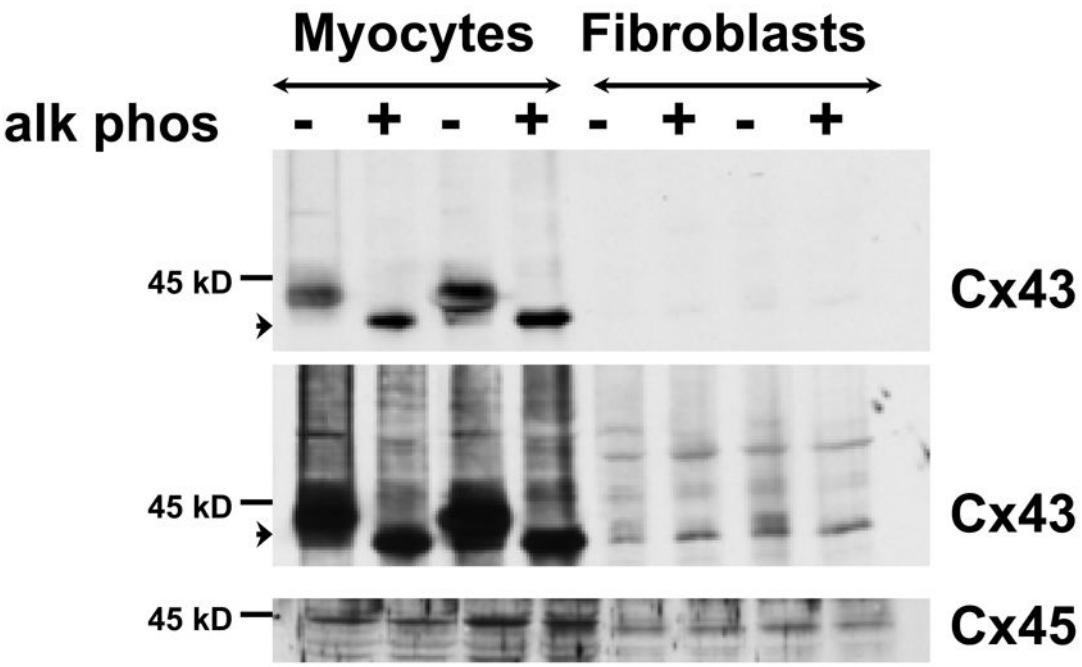

Figure 3.

Alkaline phosphatase treatment (+) of myocyte and fibroblast extracts demonstrates that dephosphorylation results in migration of a single band at 41 kD in each cell type. The top and center images are different exposures of the same membrane blotted with anti-Cx43 antibody. Two exposures are shown to illustrate alkaline phosphatase treatment in myocytes (top) and fibroblasts (center) more clearly. The bottom image shows the same membrane blotted with anti-Cx45 antiserum. Equal protein (30 μg) was loaded in each lane.

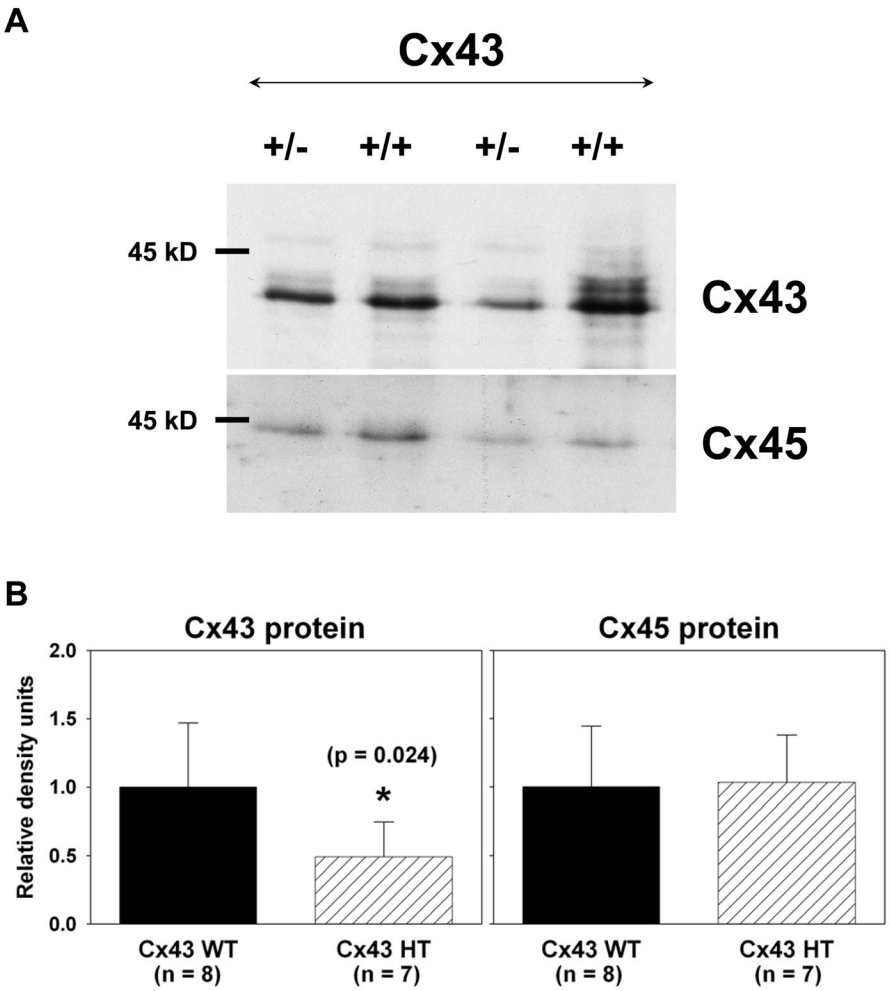

Figure 4.

Cx43 expression and intercellular coupling are reduced in Cx43-deficient cardiac fibroblasts. (A) Cx43 expression (top) is reduced in cardiac fibroblasts isolated from $Cx43^{+/-}$ hearts (+/−) compared to wild-type (+/+) as shown in this representative immunoblot. Cx45 expression (bottom) is not altered as shown in a reprobe of the same immunoblot. Equal protein (30 μg) was loaded in each lane. (B) Histograms of summarized data from fibroblasts isolated from 8 wild-type (Cx43 WT) and 7 $Cx43^{+/-}$ (Cx43 HT) hearts demonstrating that Cx43 expression was significantly reduced by ~50% in $Cx43^{+/-}$ fibroblasts. (C) Fluorescence images showing Lucifer yellow dye transfer after scrape-loading in wild-type (left) and $Cx43^{+/-}$ (Cx43 HT, right) adult murine cardiac fibroblast cultures. Outlines beside each fluorescence image represent the areas of dye transfer obtained using ImageJ software. The length of the microscopic field analyzed is shown by the double headed arrow. The total area of dye transfer was divided by this length to calculate the distance of dye transfer in μm. (D) Histograms of summarized data showing a 24% reduction in distance of dye transfer in Cx43-deficient fibroblasts.

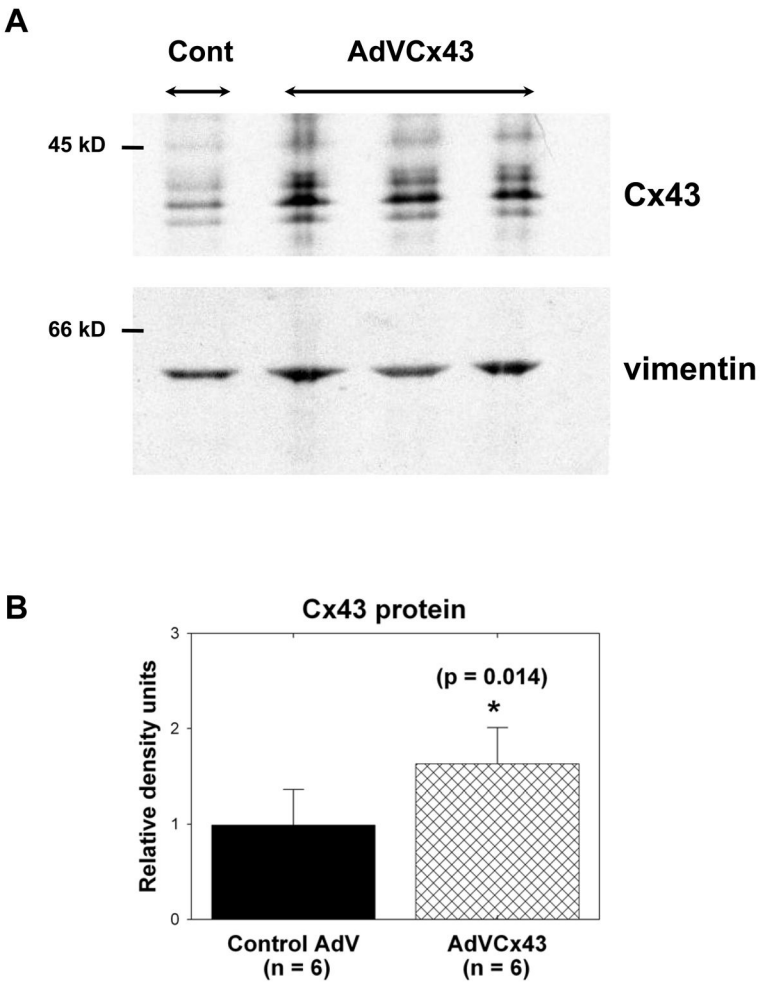

Figure 5.

AdVCx43 infection resulted in overexpression of Cx43 and increased intercellular coupling in adult cardiac fibroblasts. (A) Fibroblasts isolated from wild-type hearts treated with control adenoviral (Cont, first lane) or AdVCx43 (last three lanes) constructs (MOI 50–100), blotted with anti-Cx43 antibody (top). The same membrane was blotted with anti-vimentin antibody (bottom). Equal protein (20 μg) was loaded in each lane and Cx43 band densities were normalized to vimentin band densities. Each value was then normalized to the control values on each membrane. (B) Histograms of summarized data showing a 1.6-fold increase in Cx43 protein expression in AdVCx43-infected fibroblasts. (C) Fluorescence images showing Lucifer yellow dye transfer after scrape-loading in wild-type control adenovirus-infected (Control AdV, MOI 100, left) and AdVCx43-infected (MOI 100, right) adult murine cardiac fibroblast cultures. Outlines beside each fluorescence image represent the areas of dye transfer obtained using ImageJ software. The distance of dye transfer was calculated as described in the legend for Figure 4 and in the text. (D) Histograms of summarized data showing a 60% increase in distance of dye transfer in fibroblasts overexpressing Cx43.

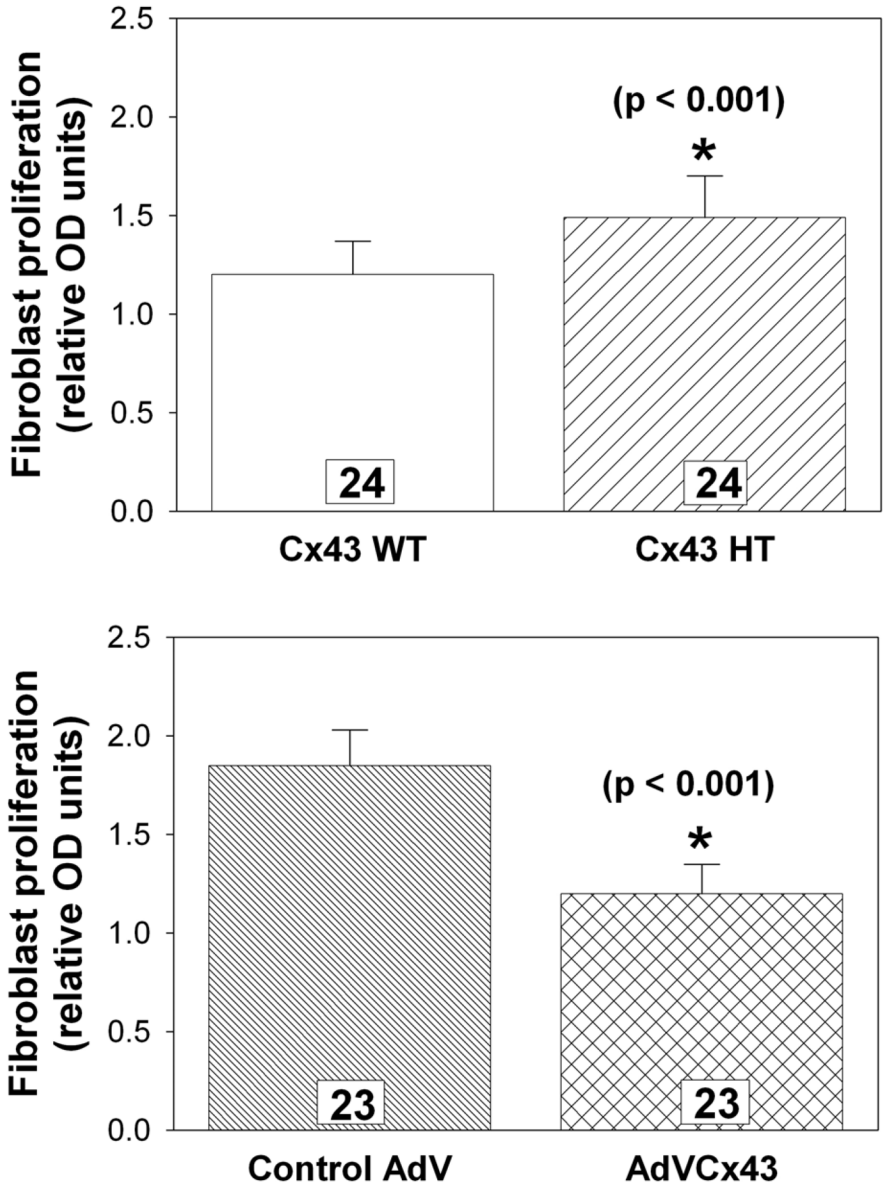

Figure 6.

Fibroblast proliferation measured by a BrdU colorimetric ELISA assay is inversely related to the level of Cx43 expression. Cx43-deficient fibroblasts (Cx43 HT) exhibit significantly ($p<0.001$) greater proliferation (top), whereas Cx43-overexpressing fibroblasts (AdVCx43) exhibit significantly ($p<0.001$) less proliferation (bottom) compared to wild-type (Cx43 WT) or control adenovirus (AdV)-infected cultures, respectively. N's are individually plated wells from 4 independent hearts for each genotype or treatment.